CONF-951033--18
SAND95-1767C

EXCITON ANNIHILATION STUDIES IN POLY(*P*-PHENYLENE VINYLENE)

V.S. Valencia, R.G. Kepler, S.J. Jacobs, and P.M. Beeson
Sandia National Laboratories, P.O. Box 5800, Albuquerque, NM 87185
P.-M. Allemond
Donnelly Corporation, 4545 E. Fort Lowell Rd, Tucson, AZ 85712

ABSTRACT

To verify the excitonic nature of the light-emitting state in PPV, fluorescence intensities and decay lifetimes were investigated as a function of excitation intensity. The results agree with the behavior predicted by the molecular exciton model. In particular, exciton-exciton annihilation causes the fluorescence intensity to saturate and the fluorescence lifetime to shorten at high exciton densities. In addition, the exciton annihilation, and thus diffusion, coefficients are found to be relatively large, even at low temperatures, indicating that exciton migration is important in PPV. These results indicate that the fluorescent (photoluminescent) state in PPV is excitonic in nature. The results argue against the band model where high mobility at reduced temperatures is not expected because the light-emitting species, neutral bipolarons, are associated with large lattice distortions.

KEYWORDS: Poly(*p*-phenylene vinylene) (PPV), Exciton, Fluorescence

1. INTRODUCTION

Since electroluminescence was first observed in poly(*p*-phenylene vinylene) (PPV) light emitting diodes (LEDs) in 1990 (1), there has been much controversy regarding the nature of the light emitting state. Various photo-excitation experiments have lead to two different pictures, the exciton (2-6) and band (7,8) models, to describe the light-emitting optical transition. The molecular exciton picture assumes that an absorbed photon creates a mobile, tightly-bound Frenkel exciton. Light is emitted when the exciton radiatively decays. The excitons are localized on segments of the PPV chain and can relax to lower energy (longer) segments in the inhomogeneously broadened absorption manifold. In the quasi-one-dimensional semiconductor band picture, photon absorption is thought to create free charge carriers in band states which rapidly relax to the band edge and then self-localize and form polarons. Light is emitted from the radiative recombination of oppositely charged polarons, or neutral bipolarons.

1.1 Exciton vs. Band Models

In reality, evidence exists to support both exciton and band pictures. In strong support of the band picture, the onset of photoconductivity in PPV coincides with the onset of optical absorption suggesting the creation of free carriers (9). However, under applied bias, a time delay exists between photogeneration and fluorescence quenching indicating an exciton dissociation process (10). In addition, absorption (11) and fluorescence (12) spectra for isolated oligo(*p*-phenylene vinylene)s are very similar to those for PPV. Since the oligomer transitions are excitonic, the similarity suggests an excitonic nature to the underlying transition in the polymer. However, the large spectral separation between the absorption and fluorescence peaks indicates a large Stokes shift as expected for polarons associated with large lattice distortions. In the exciton model, this large spectral separation is explained by exciton diffusion to longer, lower energy PPV segments in the tail of the absorption edge. Excitation below a localization threshold, where the excitons can no longer diffuse, yields a Stokes shift of only 100 cm^{-1} (2). In the band model for a disordered semiconductor, the apparent small Stokes shift is explained by relaxation of delocalized states into localized states below a mobility edge. (8) Many more arguments for and against both pictures appear in the literature. While evidence in support of an excitonic light-emitting state is strong, the evidence for polaronic carrier processes cannot be ignored.

In light of the various published results, it appears that there may be some validity to both exciton and band (polaron) pictures in PPV films. To this end, photo-induced absorption experiments indicate that some percentage of absorbed photons create excitons while the remaining percentage create spatially-indirect excitons, also referred to as neutral bipolarons, polaron pairs bound by Coulomb attraction (13-18). A possible production mechanism of these split excitons is excitation onto a chain segment shorter than the singlet exciton length (about 6 chain segments, ~40Å (5)) where it would be energetically favorable for an electron or hole to move to a segment on an adjacent chain (3,4,19). The exciton and neutral bipolaron energies must be nearly the same in this picture.

1.2 Exciton-Exciton Annihilation

The overall picture that emerges is one where both excitons and neutral bipolarons are created by absorbed photons on a subpicosecond time scale, the ratio depending on individual film characteristics. The geminate recombination of the neutral bipolarons is predominantly nonradiative and thus does not contribute significantly to fluorescence yield (17). In this picture where the light-emitting state is excitonic, fluorescence intensities and lifetimes should be profoundly influenced by bimolecular nonradiative recombination processes, or exciton-exciton annihilation, when exciton populations are very large. This can be seen in the exciton population rate equation,

$$\frac{dn}{dt} = q\alpha I_{ex} e^{-\alpha x} - \beta n - \gamma n^2 ,$$

where n is the exciton population, t is time, q is the percentage of absorbed photons creating excitons, α is the absorption coefficient at the excitation wavelength, I_{ex} is the excitation intensity, x is the position in the film, β is the unimolecular decay rate constant (the inverse of the fluorescence lifetime), and γ is the bimolecular decay rate constant, or exciton-exciton annihilation coefficient. Exciton-exciton annihilation occurs when two excitons diffuse close enough to each other to interact via dipole-dipole processes. The energy of one exciton is transferred to another resulting in the nonradiative decay of one and the promotion of the other to a higher energy level. The higher energy exciton rapidly decays nonradiatively back to the lowest electronic excited state. Thus for every "collision" between two excitons, a fluorescence photon is lost. At high exciton densities, this bimolecular process will cause fluorescence intensities to saturate and fluorescence lifetimes to shorten.

Evidence for bimolecular nonradiative recombination processes at high excitation powers in PPV was initially observed in the late 1980s (20,21). We have elaborated on these initial results by investigating PPV fluorescence intensities and lifetimes as a function of excitation intensity. Our results fit well to the solutions of the exciton population rate equation above which includes both unimolecular and bimolecular decay processes. This good agreement of our results with molecular exciton model predictions provides additional evidence that the fluorescent state in PPV is excitonic in nature. In addition, the exciton annihilation, and thus diffusion, coefficients are found to be relatively large, even at low temperatures, indicating that exciton migration is important in these materials. This argues against the band model; high mobility at reduced temperatures is not expected for neutral bipolarons because of the large lattice distortions associated with these species.

2. PPV FLUORESCENCE EXPERIMENTS

Fluorescence (photoluminescence) experiments were performed on a 1500-Å thick PPV film. The PPV precursor was synthesized by the Wessling route as discussed previously (22). The precursor was spun onto a fused silica substrate at 1000 RPM and converted at 250°C under a constant flow of forming gas (4% H_2, 96% Argon) for two hours.

The excitation intensity dependence of PPV fluorescence was studied at 77 and 295 K in vacuum ($\sim 10^{-6}$ torr) using two techniques. The fluorescence intensity was analyzed using 400-nm, 4.5-ns pulses from an Nd:YAG-pumped dye laser. The peak of the fluorescence spectrum was selected with a monochromator (~10 nm bandwidth), detected with a photomultiplier tube, and integrated using a boxcar averager. The excitation energy was measured using a Laser Precision energy meter.

In the other technique, the fluorescence lifetime was measured using time-correlated single photon counting. The 400-nm, 150-fs excitation pulses were generated by doubling the pulses from a regeneratively-amplified Ti:sapphire laser with a thin $LiNbO_3$ crystal. A double-subtractive monochromator selected a portion of the fluorescence spectrum centered at the peak for temporal analysis. The excitation power was measured with a Scientech calorimeter.

3. INTENSITY-DEPENDENT FLUORESCENCE RESULTS

The excitation intensity dependence of the fluorescence intensity at 77 and 295 K is shown in Figure 1. The ratio of the fluorescence to excitation intensities is normalized to unity. The fluorescence intensity is proportional to the excitation intensity at low excitation intensities and becomes sublinear at high excitation intensities.

Figure 2 shows the 77 and 295 K fluorescence lifetime curves at low excitation intensities where exciton annihilation processes are not expected to influence the dynamics. The 295-K curve decays faster than the 77-K curve, and both curves deviate from single exponential behavior. The instrument response of the time-correlated single photon counting apparatus is indicated by the dashed line. Fluorescence lifetime curves at 77 K for increasing excitation intensities are shown in Figure 3. The equivalent excitation intensities for the curves in Figure 3 are indicated by the arrows in Figure 1, and the legend indicates the calculated exciton densities at the front surface of the film for each curve. The lifetimes clearly become shorter at higher excitation intensities (exciton densities). Similar behavior is observed at 295 K. At exciton densities less than $5x10^{16}$ cm^{-3}, no changes in the fluorescence lifetime were observed.

4. EXCITON ANNIHILATION ANALYSIS AND DISCUSSION

These intensity-dependent fluorescence results can be fit to the appropriate solutions of the exciton population rate equation. For the nanosecond fluorescence intensity curves, steady state is assumed and the rate equation is set equal to zero, solved for the exciton density, n, and integrated over the thickness of the sample to account for the decrease in exciton density with sample thickness. Likewise, for the femtosecond fluorescence lifetime curves, the excitation term, essentially a delta function on the time scale of interest, is ignored, and the rate equation solved for n and integrated over the sample thickness.

To compare the rate equation solutions to the experimental data, the four unknowns must be quantified: q, α, β, and γ. We will initially assume that every absorbed photon creates an exciton, q=1. The absorption values at 400 nm are $2.1x10^5$ and $2.3x10^5$ cm^{-1} at 77 and 295 K, respectively. The β values are determined by fitting the experimental lifetime curves with a single exponential convolved with the instrument response function. The fits, shown with solid lines in Figure 2, indicate that the lifetimes are not pure exponentials. The intrinsic exciton lifetime, τ_o, is on the order of 1 ns in PPV (23). Nonexponential fluorescence lifetime behavior has been attributed to carbonyl-group quenching sites which provoke nonradiative exciton decay (23). PPV films are sensitive to photooxidation where carbonyl substitution occurs at the vinyl double bonds. The nonexponential dynamics of our PPV film indicate a finite carbonyl content. A stretched exponential function, indicating a distribution of exponential lifetimes depending on the varying carbonyl content in the film, yields a superior fit to the lifetime data as discussed below. However, the single exponential fits shown here are adequate to demonstrate the validity of the exciton rate equation. The fits yield β values of $5x10^9$ and $7x10^9$ sec^{-1} at 77 and 295 K, respectively.

Using these values, the exciton annihilation coefficients are determined by fitting the nanosecond fluorescence intensity curves. The fits yield relatively large γ values, $4x10^{-8}$ and $8x10^{-8}$ cm^3/sec at 77 and 295 K, respectively. In anthracene crystals, $\gamma \sim 1x10^{-8}$ cm^3/sec (24). Clearly, the nanosecond solution to the population rate equation fits the experimental data very well. In a system where q is less than 1, these values should be divided by q yielding even larger γ values. Finally, the theoretical curves predicted from the femtosecond rate equation solution, using the above values, are convolved with the instrument response curve as shown by the solid lines in Figure 3. The visually estimated spot size, needed for intensity determination, was increased slightly to obtain the best fit. Otherwise, there were no adjustable parameters. Clearly, the lifetime curves predicted by the femtosecond rate equation solution show the same trend as the experimental data, a reduction in fluorescence lifetime at higher excitation intensities.

As suggested above, the theoretical fit to the decay data is much improved if a stretched exponential decay function is used. The solution to the exciton rate equation modified for a stretched exponential decay is straight forward for the femtosecond case. However, for the nanosecond case, steady state can no longer be assumed and the solution is much more complex. While this work is currently underway and will be presented in a later paper, the results presented here, based on a single exponential decay lifetime, are sufficient to illustrate the applicability of the molecular exciton model to disordered PPV systems.

Specifically, the realistic fits of the fluorescence results to the solutions of the exciton population rate equation indicate that the light-emitting state in PPV is excitonic. The fits yield exciton annihilation coefficients which change little with temperature, only a factor of two from 77 to 295 K. This small change indicates that the excitons are associated with only a small lattice distortion. When the excitons diffuse with a mean free path small compared to the distance *R* at which they interact, assumed here to be the exciton delocalization length, ~40 Å, the exciton annihilation coefficient

$$\gamma = 8\pi DR \ \alpha \ e^{-\frac{\Delta E}{kT}},$$

where *D* is the diffusion coefficient. Both exciton annihilation and diffusion are thermally activated processes with activation energy ΔE. Determining the activation energy using the γ values at 77 and 295 K yields ΔE=6 meV (50 cm^{-1}). Within a factor of two, this activation energy agrees with the Stokes shift measured by Raucher, *et. al.* (2) indicating that the exciton is dressed with a small lattice distortion. ΔE could also be considered a measure of the (polaronic) exciton binding energy. In the band picture, the neutral bipolarons responsible for light emission are expected to be associated with much larger lattice distortions than observed here.

As expected when only small lattice distortions are associated with excitons, the diffusion coefficients are relatively large, even at low temperatures, 0.004 and 0.008 cm^2/sec at 77 and 295 K, respectively, indicating that exciton migration is important in these materials. Again, this argues against the band model where high mobility at reduced temperatures is not expected for neutral bipolaron light-emitting species due to their large lattice distortions.

Exciton mobility is an important issue in electroluminescent LED operation. The relatively large exciton diffusion radius in PPV, $r=(D\ \tau_o)^{1/2}$ (~300 Å at room temperature), should be considered when designing LED structures. That is, the charge carrier recombination zone should be located far from possible quenching interfaces for maximum device efficiency. Electroluminescence-detected magnetic resonance studies indicate that fusion of charged polarons to singlet excitons, which then decay radiatively, is responsible for electroluminescence in PPV LEDs (25). Assuming an exciton-to-photon conversion efficiency of 10%, the exciton density required to achieve 100,000 cd/m^2 of green electroluminescence is about 10^{14} cm^{-3}. Exciton-exciton annihilation processes become important at densities of about 10^{16} cm^{-3} and are thus not expected to influence LED performance.

5. CONCLUSIONS

We have shown that the excitation intensity dependencies of PPV fluorescence intensities and lifetimes agree well with behavior predicted by the molecular exciton model. Exciton-

exciton annihilation causes the fluorescence intensity to saturate and the fluorescence lifetimes to shorten at high exciton densities. These results indicate that excitons are the light-emitting states in PPV, but do not support the band picture where the light-emitting species are neutral bipolarons.

6. ACKNOWLEDGMENTS

Assistance with the femtosecond laser experiment by M.B. Sinclair is gratefully acknowledged. This work was supported by the United States Department of Energy under Contract Number DE-AC04-94AL85000.

7. REFERENCES

1. J.H. Burroughes, D.D.C. Bradley, A.R. Brown, R.N. Marks, K. Mackay, R.H. Friend, P.L. Burns and A.B. Holmes, Nature **347**, 539 (1990).
2. U. Rauscher, H. Bässler, D.D.C. Bradley and M. Hennecke, Phys. Rev. B **42**, 9830 (1990).
3. M. Gailberger and H. Bässler, Phys. Rev.B **44**, 8643 (1991).
4. H. Bässler, M. Gailberger, R.F. Mahrt, J.M. Oberski and G. Weiser, Synth. Met. **49-50**, 341 (1992).
5. L.J. Rothberg, J.W.P. Hsu, W.L. Wilson, T.M. Jedju, M. Yan and B.R. Hsieh, SPIE Proceedings **1910**, 122 (1993).
6. H. Antoniadis, B.R. Hsieh, M.A. Abkowitz, S.A. Jenekhe and M. Stolka, Mol. Cryst. Liq. Cryst. **256**, 381 (1994).
7. T.W. Hagler, K. Pakbaz, K.F. Voss and A.J. Heeger, Phys. Rev. B **44**, 8652 (1991).
8. D. McBranch, F.H. Long, T.W. Hagler, J.M. Robinson, B.I. Swanson, K. Pakbaz, A.J. Heeger, S. Schricker and F. Wudl, Mol. Cryst. Liq. Cryst. **256**, 499 (1994).
9. K. Pakbaz, C.H. Lee, A.J. Heeger, T.W. Hagler and D. McBranch, Synth. Met. **64**, 295 (1994).
10. R. Kersting, U. Lemmer, M. Deussen, H.J. Bakker, R.F. Mahrt, H. Kurz, V.I. Arkhipov, H. Bässler and E.O. Göbel, Phys. Rev. Lett. **73**, 1440 (1994).
11. B. Tian, G. Zerbi, R. Schenk and K. Müllen, J. Chem. Phys. **95**, 3191 (1991).
12. R. Mahrt, J. Yang, A. Greiner, H. Bässler and D.D.C. Bradley, Makromol. Chem. Rapid Commun. **11**, 415 (1990).
13. D.C.C. Bradley, R.H. Friend, F.L. Pratt, K.S. Wong, W. Hayes, H. Lindenberger and S. Roth, in *Electronic Properties of Conjugated Polymers* H. Kuzmany, M. Mehring and S. Roth, Eds. (Springer-Verlag, New York, 1987), vol. 76, pp. 113-117.
14. D.D.C. Bradley, N.F. Colaneri and R.H. Friend, Synth. Met. **29**, E121 (1989).
15. N.F. Colaneri, D.D.C. Bradley, R.H. Friend and C.W. Spangler, in *Springer Series in Solid-State Sciences* H. Kuzmany, M. Mehring and S. Roth, Eds. (Springer-Verlag, Berlin, 1989), vol. 91, pp. 91-95.

16. E.L. Frankevich, A.A. Lymarev, I. Sokolik, F.E. Karasz, S. Blumstengel, R.H. Baughman and H.H. Horhold, Phys. Rev. B **46**, 9320 (1992).

17. M. Yan, L.J. Rothberg, F. Papadimitrakopoulos, M.E. Galvin and T.M. Miller, Phys. Rev. Lett. **72**, 1104 (1994).

18. J.W.P. Hsu, M. Yan, T.M. Jedju, L.J. Rothberg and B.R. Hsieh, Phys. Rev. B **49**, 712 (1994).

19. E.M. Conwell and H.A. Mizes, Mol. Cryst. Liq. Cryst. **256**, 27 (1994).

20. D.D.C. Bradley, R.H. Friend and W.J. Feast, Synth. Metals **17**, 645 (1987).

21. K.S. Wong, D.D.C. Bradley, W. Hayes, J.F. Ryan, R.H. Friend, H. Lindenberger and S. Roth, J. Phys. C: Solid State Phys. **20**, L187 (1987).

22. R.G. Kepler, V.S. Valencia, S.J. Jacobs and J.J. McNamara, Synth. Met. *in press*.

23. M. Yan, L.J. Rothberg, F. Papadimitrakopoulos, M.E. Galvin and T.M. Miller, Phys. Rev. Lett. **73**, 744 (1994).

24. R.G. Kepler, in *Treatise on Solid State Chemistry* N. B. Hannay, Eds. (Plenum, New York, 1976), vol. 3 Crystalline and Noncrystalline Solids, pp. 615-678.

25. L.S. Swanson, J. Shinar, A.R. Brown, D.D.C. Bradley, R.H. Friend, P.L. Burn, A. Kraft and A.B. Holmes, Phys. Rev. B **46**, 15072 (1992).

16. E.L. Frankevich, A.A. Lymarev, I. Sokolik, F.E. Karasz, S. Blumstengel, R.H. Baughman and H.H. Horhold, Phys. Rev. B **46**, 9320 (1992).

17. M. Yan, L.J. Rothberg, F. Papadimitrakopoulos, M.E. Galvin and T.M. Miller, Phys. Rev. Lett. **72**, 1104 (1994).

18. J.W.P. Hsu, M. Yan, T.M. Jedju, L.J. Rothberg and B.R. Hsieh, Phys. Rev. B **49**, 712 (1994).

19. E.M. Conwell and H.A. Mizes, Mol. Cryst. Liq. Cryst. **256**, 27 (1994).

20. D.D.C. Bradley, R.H. Friend and W.J. Feast, Synth. Metals **17**, 645 (1987).

21. K.S. Wong, D.D.C. Bradley, W. Hayes, J.F. Ryan, R.H. Friend, H. Lindenberger and S. Roth, J. Phys. C: Solid State Phys. **20**, L187 (1987).

22. R.G. Kepler, V.S. Valencia, S.J. Jacobs and J.J. McNamara, Synth. Met. *in press*.

23. M. Yan, L.J. Rothberg, F. Papadimitrakopoulos, M.E. Galvin and T.M. Miller, Phys. Rev. Lett. **73**, 744 (1994).

24. R.G. Kepler, in *Treatise on Solid State Chemistry* N. B. Hannay, Eds. (Plenum, New York, 1976), vol. 3 Crystalline and Noncrystalline Solids, pp. 615-678.

25. L.S. Swanson, J. Shinar, A.R. Brown, D.D.C. Bradley, R.H. Friend, P.L. Burn, A. Kraft and A.B. Holmes, Phys. Rev. B **46**, 15072 (1992).

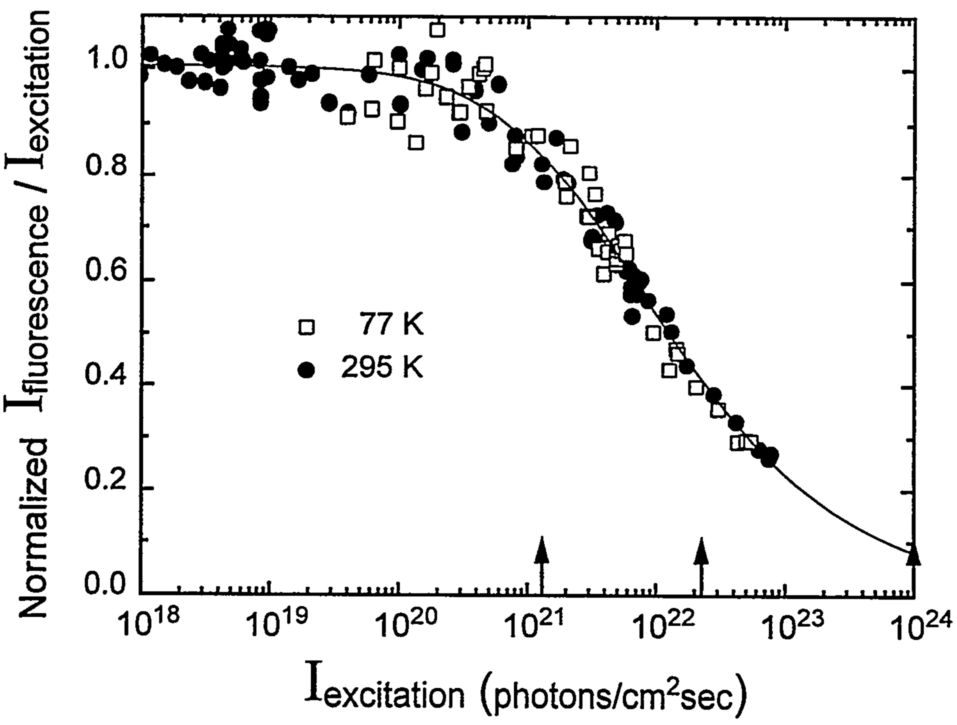

Figure 1. Excitation intensity dependence of PPV fluorescence intensity.

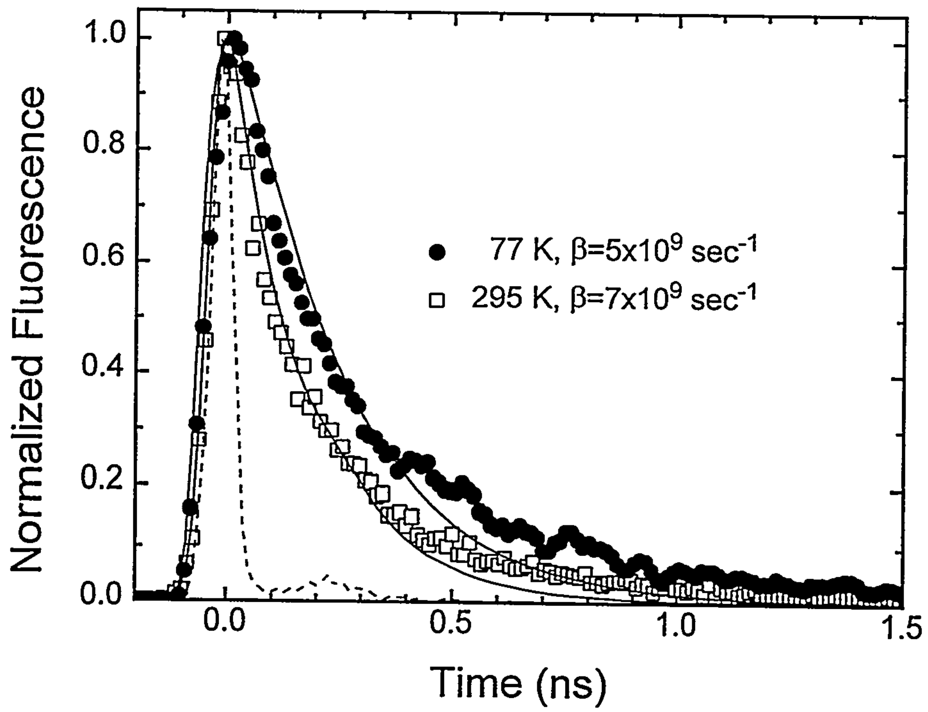

Figure 2. PPV fluorescence lifetimes as low excitation intensities.

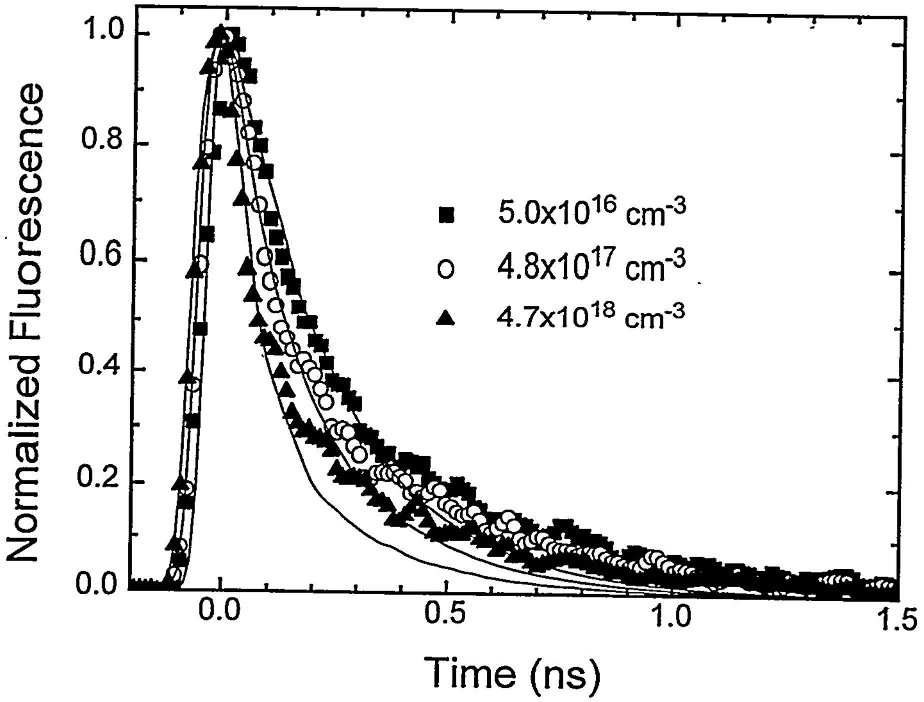

Figure 3. PPV fluorescence lifetimes at high excitation intensities at 77 K.